

Confronting the Fermi Line with LHC data: an Effective Theory of Dark Matter Interaction with Photons

Andy Nelson,¹ Linda M. Carpenter,² Randel Cotta,¹ Adam Johnstone,¹ and Daniel Whiteson¹

¹*Department of Physics and Astronomy, University of California, Irvine, CA 92697*

²*The Ohio State University, Columbus, OH*

We describe an effective theory of interaction between pairs of dark matter particles and pairs of photons. Such an interaction could accomodate $\chi\bar{\chi} \rightarrow \gamma\gamma$ processes which might be the cause of the observed feature in the FermiLAT spectrum, as well as $\gamma^*/Z \rightarrow \gamma\chi\bar{\chi}$ processes, which would predict excesses at the LHC in the $\gamma + \cancel{E}_T$ final-state. We reinterpret an ATLAS $\gamma + \cancel{E}_T$ analysis and the observed Fermi feature in the parameter space of our new effective theory to assess their consistency.

PACS numbers:

Introduction

Strong evidence for dark matter exists in the form of precise measurements of galactic rotation curves and gravitational lensing, but its nature is still largely a mystery [1]. A vigorous experimental program seeks to identify the particle nature of weakly-interacting cold dark matter, χ , by looking for the scattering of heavy nuclei by local dark matter, or annihilation in space of dark matter pairs into standard model particles. Recently, a statistically significant peak was observed in the Fermi-LAT photon spectrum, which can be interpreted as $\chi\chi \rightarrow \gamma\gamma$ [2], though concerns have been raised about its possible origin as an instrumental artifact [3–5].

High energy particle accelerators provide another experimental probe, as they can directly produce pairs of dark matter particles, independent of the local or galactic dark matter density. Pairs of dark matter particles produced at colliders are, however, invisible to the detectors. A fruitful approach has been to consider the case in which a standard model particle is emitted as initial state radiation preceeding the dark matter production, see the top of Fig. 1. The final state signature is then a single reconstructed object (jet [6, 7], photon [8, 9], Z boson [10, 11] etc) with no object to balance its transverse momentum, leading to large missing transverse momentum (\cancel{E}_T).

The production of dark matter particles is usually assumed to be due to an interaction between the dark matter particles χ and the primary constituents of the collider initial state (q or g). The precise nature of this interaction is not known, but a useful general formalism is provided by effective field theories [12–14], which are strictly speaking valid only when the coupling occurs through states which are heavy compared with the typical energies involved ($\sim \cancel{E}_T$) and can be integrated out to give an effective four-fermion operator.

Recently [10, 15], this has been extended to consider the case of an effective field theory which couples the

dark matter fields to electroweak bosons rather than to the fermionic initial state. For such interactions the Z boson+ \cancel{E}_T final state would be one of the unique strategies for searching for dark matter at colliders.

In this paper, we extend this line of thought to the $\gamma + \cancel{E}_T$ final state, reinterpreting the ATLAS analysis which sets limits on theories of quark-WIMP effective interactions in terms of theories of photon-WIMP effective interactions (see the bottom of Fig. 1), working in an effective theory framework with a very simple parameter space.

This class of interactions is of particular interest as collider production of $\gamma + \cancel{E}_T$ via $\gamma^*/Z \rightarrow \gamma\chi\bar{\chi}$ is tied directly to the cross-section of putative monochromatic γ -ray signals via $\chi\bar{\chi} \rightarrow \gamma\gamma$, allowing the confrontation of LHC and Fermi-LAT data in the parameter space of our new effective theory. In this paper, we place bounds from $\gamma + \cancel{E}_T$ in the space of parameters that would generate a signal at Fermi-LAT.

Model

We consider effective operators through which pairs of neutral stable particles may couple to photons and possibly also the Z boson. We consider operators where the DM particles involved are scalars, as well as those in which they are fermions.

The most relevant (lowest-dimensional) operators involving scalar DM particles, ϕ , are the dimension-6 operators:

$$\mathcal{L} = \frac{1}{\Lambda_{B1,2}^2} \bar{\phi}\phi \sum_i k_i F_i^{\mu\nu} F_{\mu\nu}^i + \frac{1}{\Lambda_{B3,4}^2} \bar{\phi}\phi \sum_i k_i F_i^{\mu\nu} \tilde{F}_{\mu\nu}^i \quad (1)$$

where F_i , $i = 1, 2$ are the field strengths of the SM $U(1)$, $SU(2)$ gauge groups. Here and below, we label the effective cut-offs of distinct operators Λ_{Bi} or Λ_{Ci} using the

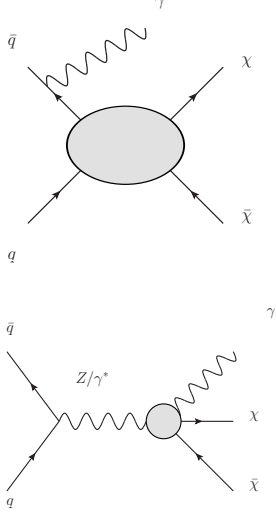


FIG. 1: Representative diagrams for production of dark matter pairs ($\chi\bar{\chi}$) associated with a photon in theories where dark matter interacts with quarks (top) or directly with weak boson pairs (bottom). The latter are those that we consider in this work.

notation of Ref. [16]. Note that in the second operator, the dual field strength tensor appears.

Similarly, the most relevant operators involving fermionic DM, χ , are the dimension-7 operators:

$$\mathcal{L} = \frac{1}{\Lambda_{C1,2}^3} \bar{\chi}\chi \sum_i k_i F_i^{\mu\nu} F_{\mu\nu}^i + \frac{1}{\Lambda_{C3,4}^3} \bar{\chi}\chi \sum_i k_i F_i^{\mu\nu} \tilde{F}_{\mu\nu}^i \quad (2)$$

and

$$\mathcal{L} = \frac{1}{\Lambda_{C5,6}^3} \bar{\chi}\gamma^5\chi \sum_i k_i F_i^{\mu\nu} F_{\mu\nu}^i + \frac{1}{\Lambda_{C7,8}^3} \bar{\chi}\gamma^5\chi \sum_i k_i F_i^{\mu\nu} \tilde{F}_{\mu\nu}^i, \quad (3)$$

where here there are more operators than in the scalar case as the fermionic bilinears can have different Lorentz structures. While the differences in collider limits on these operators are small (they differ only in their phase-space structure), the differences in their cosmic annihilation rates are substantial, as C1-C4 are velocity suppressed, $\langle\sigma v\rangle \sim v^2$, while C5-C8 are not.

Given the form of the operators in Eqns. 1-3 the couplings of the DM to various pairs of electroweak gauge

bosons are simply related by gauge symmetry:

$$g_{WW} = \frac{2k_2}{s_w^2 \Lambda^{2-3}} \quad (4)$$

$$g_{ZZ} = \frac{1}{4s_w^2 \Lambda^{2-3}} \left(\frac{k_1 s_w^2}{c_w^2} + \frac{k_2 c_w^2}{s_w^2} \right) \quad (5)$$

$$g_{\gamma\gamma} = \frac{1}{4c_w^2} \frac{k_1 + k_2}{\Lambda^{2-3}} \quad (6)$$

$$g_{Z\gamma} = \frac{1}{2s_w c_w \Lambda^{2-3}} \left(\frac{k_2}{s_w^2} - \frac{k_1}{c_w^2} \right), \quad (7)$$

where s_w and c_w are the sine and cosine of the weak mixing angle, respectively.

The parameters k_1 and k_2 control the relative couplings to electro-weak gauge bosons, but the fact that the couplings of pairs of DM particles to pairs of electro-weak gauge bosons are not all independent will be very important here. The ratios of the couplings to the four possible two boson final states are simply determined by two parameters (*e.g.*, the WW coupling can be turned off if $k_2 = 0$ while the ZZ coupling is non-zero as long as either $k_1 \neq 0$ or $k_2 \neq 0$). The total cross-sections can be described in terms of three parameters: the ratios $k_{1,2}/\Lambda$ and the mass of the DM. As one moves around in this space the ratios of collider mono-boson production in various channels will change (along with the kinematics of such production, *e.g.*, the shape of the \cancel{E}_T spectrum). There are also obviously regions of $k_{1,2}$ where interference between the underlying diagrams can completely suppress these interactions. This important fact will be reflected in our conclusions below.

In general one can write other operators involving the WW or ZZ gauge bosons at the same level in naive operator dimension¹ but the relation between the coefficients of our operators Eqns. 1-3 and of these other operators are not related by any symmetry of the Standard Model and so are UV model-dependent.

Experimental Search

The ATLAS experiment at the LHC has placed limits on dark matter production in the $\gamma + \cancel{E}_T$ channel [8], where the dark matter fields couple to quark initial states and the photon has been emitted as initial state radiation. These limits were derived from 4.6 fb⁻¹ of data produced in pp collisions at $\sqrt{s} = 7$ TeV. The full selection is as follows:

- 1 photon, $p_T > 150$ GeV
- $\cancel{E}_T > 150$ GeV
- ≤ 1 jet with $p_T > 30$ GeV
- $\Delta\phi(\gamma, \cancel{E}_T) > 0.4$

¹ One can write even lower-dimensional operators, *e.g.*, the Higgs Portal $|\phi|^2 V^2$ or $\bar{\chi}\chi V^2$ operators, but these aren't even $SU(2) \times U(1)$ invariant and so must clearly be related to the couplings of our operators in a UV model-dependent fashion.

Background source	Events		
$Z(\rightarrow \nu\nu)\gamma$	93	± 16	± 8
$Z/\gamma^*(\rightarrow \ell\ell)\gamma$	0.4	± 0.2	± 0.1
$W(\rightarrow \ell\nu)\gamma$	24	± 5	± 2
$W/Z+\text{jets}$	18	± 6	
Top	0.07	± 0.07	± 0.01
Diboson	0.3	± 0.1	± 0.1
$\gamma+\text{jets}$ and multi-jet	1.0	± 0.5	
Total	137	± 18	± 9
Data		116	

TABLE I: Breakdown of the number of data and background events as measured in the ATLAS mono-photon result [8]. The first uncertainty is statistical and the second is systematic, except in the case of $W/Z+\text{jets}$, $\gamma+\text{jets}$, and multi-jet where the total uncertainty is quoted.

• $\Delta\phi(j_1, \cancel{E}_T) > 0.4$

• No electrons (muons) with $p_T > 20$ GeV and $|\eta| < 2.47$ ($p_T > 10$ GeV and $|\eta| < 2.4$)

The results are consistent with the Standard Model expectation, as shown in Table I.

Using the CLs method [17, 18], the ATLAS measurement constrains the number of non-Standard Model events to be $N < 36$ at the 95% confidence level. In order to reinterpret these results in terms of interactions with electroweak bosons we must extract cross-section limits. This can be done with the relation:

$$\sigma = \frac{N}{\mathcal{L} \times \epsilon} \quad (8)$$

where σ is the cross section, N is the number of events, \mathcal{L} is the luminosity, ϵ is the total selection efficiency.

Signal Efficiency and Limits

We generate events in this model using MADGRAPH5 [19]. The efficiency for our signal events to survive the ATLAS event selection is estimated by breaking the complete efficiency into two parts: fiducial efficiency of the selection criteria (ϵ_{fid}) and object reconstruction efficiency ϵ_{reco} . The fiducial efficiency can be reliably estimated using parton-level simulated event samples. The object reconstruction efficiency depends on the details of the detector performance, but is largely independent of the model. We generate mono-photon ISR events using the same configuration as the ATLAS analysis, measure the fiducial efficiency for each operator, and use the reported ATLAS total efficiencies to deduce the object reconstruction efficiency. This allows us to estimate the total efficiency for our new signal events.

The critical kinematic quantity is the missing transverse momentum. Figure 2 shows the distributions for a few choices of k_1, k_2 and m_χ .

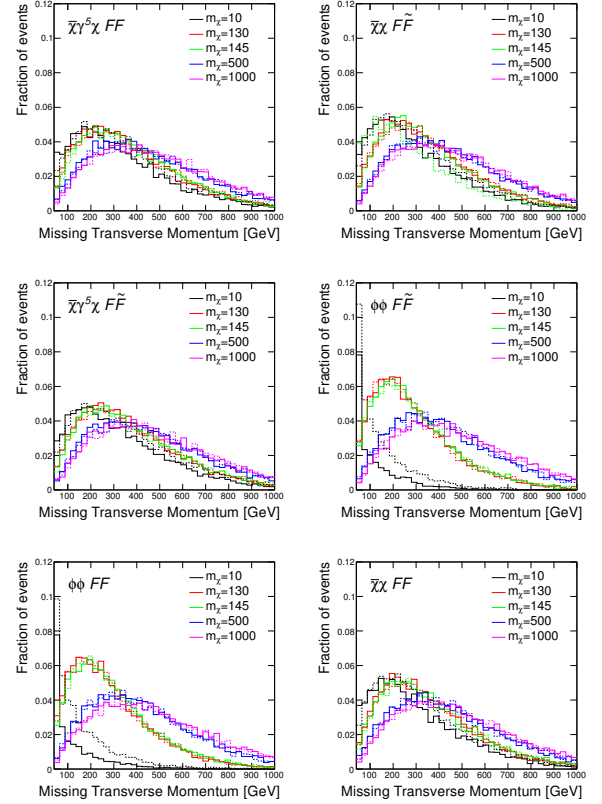


FIG. 2: Distributions of \cancel{E}_T in simulated $\gamma + \cancel{E}_T$ events in pp collisions at the LHC for several choices of m_χ and $k_1, k_2 = 0.5, 0.5$ (solid) or $1, 0$ (dashed).

Limits on the cross section are shown as a function of m_χ for several choices of k_1, k_2 in Fig. 3. As the cross section depends on the suppression scale Λ , limits on the cross section can be translated into limits on Λ , see Figs 4, 5.

We observe (Fig. 3) that the limits on light fermionic χ are much tighter than those on light scalar ϕ DM, a feature that is obviously due to the differences in \cancel{E}_T spectra (Fig. 2). It is not hard to understand these differences as, in the limit of massless χ , the fact that the fermionic operators are dimension-7 and the scalar operators are dimension-6 means that the cross-sections in the fermionic case must scale with a higher power of the momenta involved², and hence the photon p_T . The resulting cross-section is relatively suppressed as $p_T \rightarrow 0$ and is enhanced compared to the scalar case in the large p_T tail.

² Terms that don't scale with momenta are much smaller, $\mathcal{O}(m_\chi^2)/s$, i.e., they are "helicity suppressed."

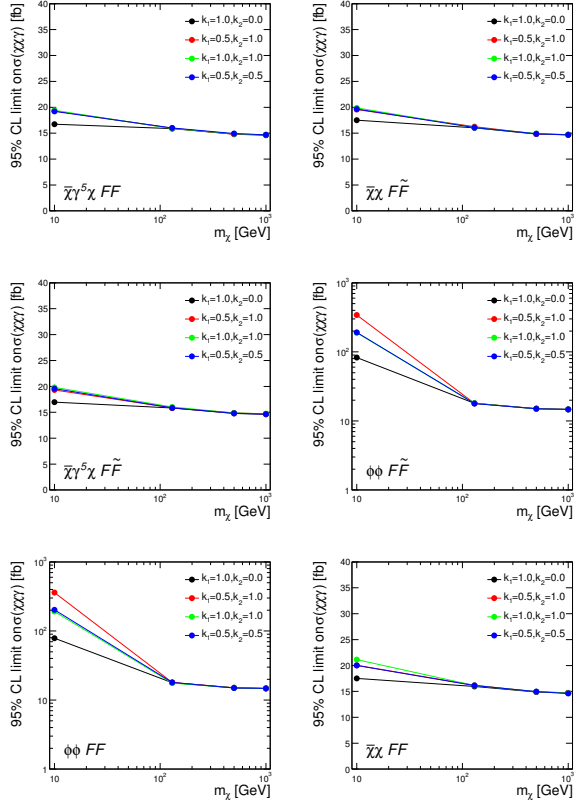


FIG. 3: Limits on $\sigma(pp \rightarrow \gamma + \cancel{E}_T)$ for several values of m_χ and k_1, k_2 .

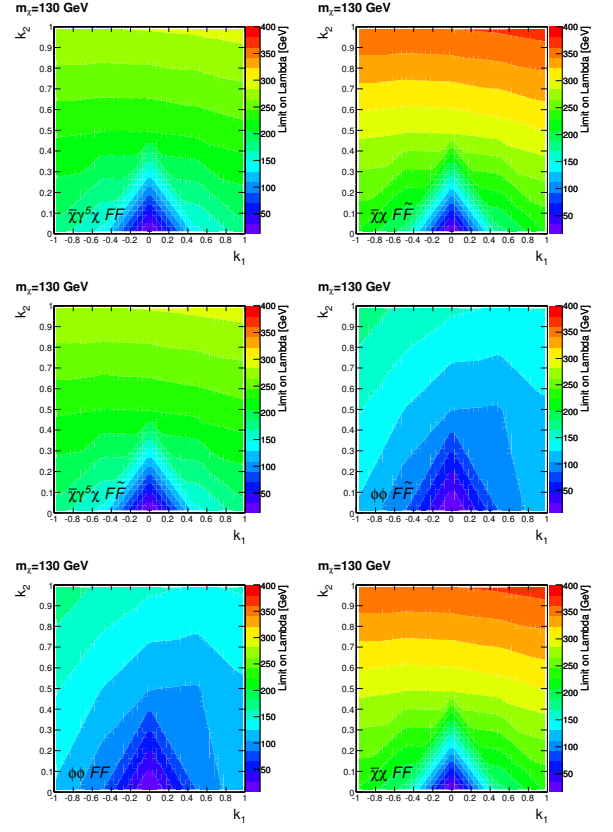


FIG. 4: Limits on Λ from $\gamma + \cancel{E}_T$ events at the LHC, with $m_\chi = 130$ GeV as a function of k_1, k_2 .

Gamma-Ray Lines from our Operators

Line Rates

For fermionic dark matter (χ), the only operators that will give sizeable annihilation rates to the $\gamma\gamma$ and γZ final states are those which are not velocity suppressed ($\bar{\chi}\chi \sim v^2$, with $v \sim 10^{-3}$). The relevant operators here are C5-C8. In the case of scalar dark matter (ϕ), none of the operators mentioned above, B1-B4, are suppressed.

Annihilation rates are straightforward to calculate for these operators, see *e.g.*, Ref. [16] for a recent accounting of such calculations. In terms of our parameterization we

find:

$$\langle\sigma v\rangle_{B1,2}^{\gamma\gamma} = \frac{2m_\chi^2}{\pi\Lambda_s^4} (k_1 c_w^2 + k_2 s_w^2)^2 \quad (9)$$

$$\langle\sigma v\rangle_{B1,2}^{\gamma Z} = \frac{3(4m_\chi^2 - m_Z^2)^3 c_w^2 s_w^2}{64\pi m_\chi^4 \Lambda_s^4} (k_1 - k_2)^2 \quad (10)$$

$$\langle\sigma v\rangle_{C5,6}^{\gamma\gamma} = \frac{4m_\chi^4}{\pi\Lambda_{f5}^6} (k_1 c_w^2 + k_2 s_w^2)^2 \quad (11)$$

$$\langle\sigma v\rangle_{C5,6}^{\gamma Z} = \frac{3(4m_\chi^2 - m_Z^2)^3 c_w^2 s_w^2}{32\pi m_\chi^2 \Lambda_{f5}^6} (k_1 - k_2)^2 \quad (12)$$

$$\langle\sigma v\rangle_{C7,8}^{\gamma\gamma} = \frac{8m_\chi^4}{\pi\Lambda_{f5}^6} (k_1 c_w^2 + k_2 s_w^2)^2 \quad (13)$$

$$\langle\sigma v\rangle_{C7,8}^{\gamma Z} = \frac{(4m_\chi^2 - m_Z^2)^3 c_w^2 s_w^2}{4\pi m_\chi^2 \Lambda_{f5}^6} (k_1 - k_2)^2. \quad (14)$$

Numerical annihilation rates for our operators are sketched in Figure 6.

Collider Bounds and the FermiLAT line

Assuming that the observed feature at $E_\gamma \approx 130$ GeV in the FermiLAT photon spectrum is a monochromatic

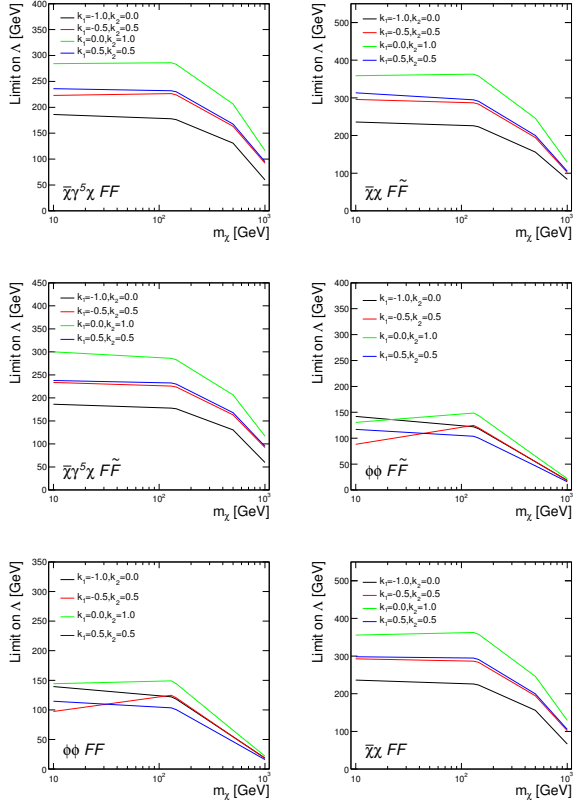


FIG. 5: Limits on Λ as a function of m_χ for several choices of k_1, k_2 .

gamma-ray line due to dark-matter annihilation, the measurement of the annihilation cross-section selects a region of parameter space of our operators and allows for a specific prediction for a collider signal.

We first determine the regions of parameter space that give the line signal under two different hypotheses: $m_{DM} = 130$ GeV with $\langle\sigma v\rangle_{\gamma\gamma} = 10^{-27} \text{cm}^3 \text{s}^{-1}$, and $m_{DM} = 145$ GeV with $\langle\sigma v\rangle_{\gamma Z} = 10^{-27} \text{cm}^3 \text{s}^{-1}$. This gives us a surface $\Lambda = \Lambda_{\text{line}}(k_i)$ which generates one of these lines and can be immediately compared to the collider excluded region $\Lambda \leq \Lambda_{\text{excl}}(k_i)$. The resulting allowed regions are shown in Figures 7-8.

For both classes of DM we find that the desired line cross-section can be obtained for approximately electroweak-scale values of Λ over most of the k_1 vs. k_2 plane. Since the cross-sections leading to $\gamma\gamma$ and γZ have different dependences on our k_1 and k_2 parameters (Eqn. 14), our Λ contours are arranged quite differently for the different final states in this plane. The Λ values required to make an observable line drop sharply in regions where the underlying B and W^0 amplitudes interfere: $k_1 = -t_w^2 k_2$ for $\gamma\gamma$ and $k_1 = k_2$ for γZ .

We observe, as expected, that our mono-photon bounds rule out the bulk of these interference regions in our parameter space, leaving only the parameter space

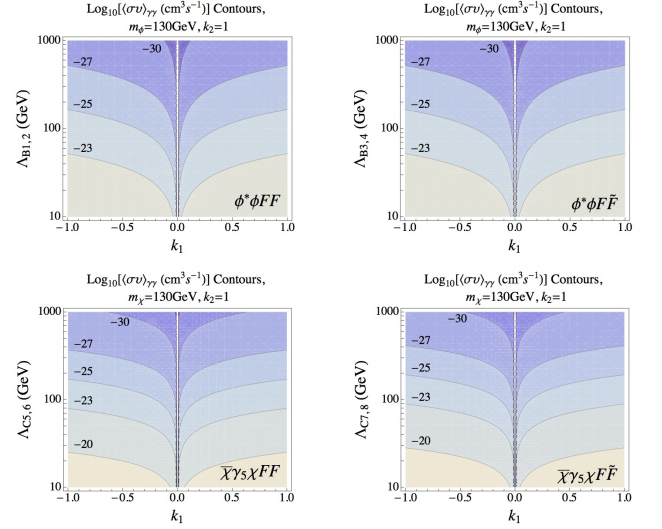


FIG. 6: Annihilation rates for our (four unsuppressed) operators. We fix $m_{DM} = 130$ GeV and $k_2 = 0$ here for illustration.

in the limit when both $k_{1,2} \approx 0$. As noted above, the observed limits on operators with fermionic DM are relatively strong when compared with those on operators with scalar DM. In approximate language, the bounds on scalar operators reach $\Lambda \lesssim 150$ GeV (a number that is small compared to the electroweak vev) while bounds on fermionic operators reach Λ values at the several hundreds of GeV levels (of the order of the electroweak vev). This explains our observation in Figs. 7-8 that the collider bounds on our scalar operators exclude essentially only regions of parameter space where some amount of tuning of k_1 and k_2 happens to reduce Λ much below the weak scale (*i.e.*, the interference regions), while collider bounds on the fermionic operators reach more general parts of our parameter space.

Conclusions

In this work we have derived constraints on dark matter interactions with photons in the context of a simply parameterized effective theory framework. $\gamma + \cancel{E}_T$ bounds derived by the ATLAS collaboration for dark matter interactions with quarks were recast to find bounds on our model for both scalar and fermionic dark matter scenarios. The kinematic differences in the two classes of DM give bounds on the dimensionful scale of the effective operators that is more tightly constraining for fermionic DM than for the scalar case, roughly $\Lambda \gtrsim 300$ GeV and $\Lambda \gtrsim 150$ GeV, respectively.

We have also investigated the interplay between the collider data and that from indirect detection searches for the energetic products of dark matter annihilation in the galaxy. A putative FermiLAT signal of DM annihilations to monochromatic gamma-rays results from our operator

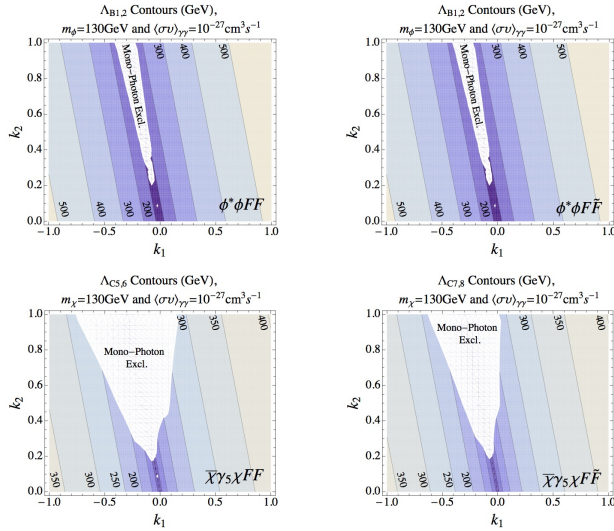


FIG. 7: Contours of Λ necessary for $m_{DM} = 130 \text{ GeV}$ and $\langle\sigma v\rangle_{\gamma\gamma} = 10^{-27} \text{ cm}^3 \text{ s}^{-1}$ for various operators in the k_2 vs. k_1 plane. Unshaded regions are excluded by our monophoton analysis.

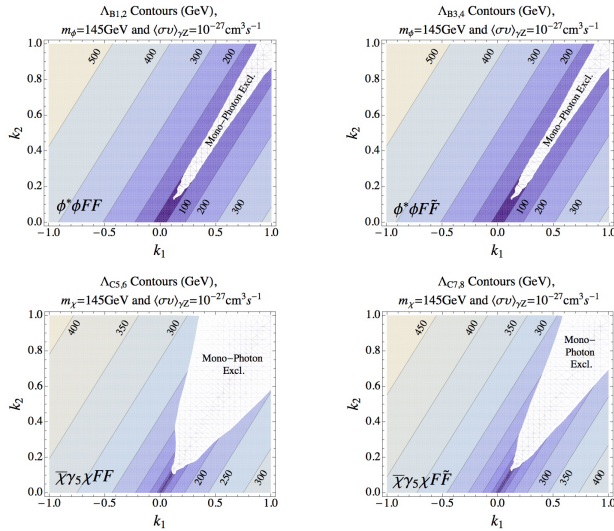


FIG. 8: As in Figure 7 except for a scenario with $m_{DM} = 145 \text{ GeV}$ and $\langle\sigma v\rangle_{\gamma Z} = 10^{-27} \text{ cm}^3 \text{ s}^{-1}$.

setup on a particular subspace of its parameters. We have described collider constraints on this subspace, finding that, although much of parameter space can be excluded by the collider search, most of the space remains viable.

Acknowledgements

We acknowledge useful conversations with Tim Tait. DW and AN are supported by grants from the Department of Energy Office of Science. RC greatly acknowledges the hospitality of the KITP and was supported in part by the National Science Foundation under PHY-

0970173 and PHY11-25915.

- [1] G. Bertone, D. Hooper, J. Silk, Phys. Rept. **405**, 279 (2005) [arXiv:0404175 [hep-ph]].
- [2] C. Weniger, AIP Conf. Proc. **1505**, 470 (2012) [arXiv:1210.3013 [astro-ph.HE]].
- [3] D. Whiteson, JCAP **1211**, 008 (2012) [arXiv:1208.3677 [astro-ph.HE]].
- [4] D. P. Finkbeiner, M. Su and C. Weniger, JCAP **1301**, 029 (2013) [arXiv:1209.4562 [astro-ph.HE]].
- [5] D. Whiteson, arXiv:1302.0427 [astro-ph.HE].
- [6] G. Aad *et al.* [ATLAS Collaboration], JHEP **1304**, 075 (2013) [arXiv:1210.4491 [hep-ex]].
- [7] S. Chatrchyan *et al.* [CMS Collaboration], JHEP **1209**, 094 (2012) [arXiv:1206.5663 [hep-ex]].
- [8] G. Aad *et al.* [ATLAS Collaboration], arXiv:1209.4625 [hep-ex].
- [9] S. Chatrchyan *et al.* [CMS Collaboration], Phys. Rev. Lett. **108**, 261803 (2012) [arXiv:1204.0821 [hep-ex]].
- [10] L. M. Carpenter, A. Nelson, C. Shimm, T. M. P. Tait and D. Whiteson, arXiv:1212.3352 [hep-ex].
- [11] N. F. Bell, J. B. Dent, A. J. Galea, T. D. Jacques, L. M. Krauss and T. J. Weiler, Phys. Rev. D **86**, 096011 (2012) [arXiv:1209.0231 [hep-ph]].
- [12] J. Goodman, M. Ibe, A. Rajaraman, W. Shepherd, T. M. P. Tait and H. -B. Yu, Phys. Rev. D **82**, 116010 (2010) [arXiv:1008.1783 [hep-ph]].
- [13] M. Beltran, D. Hooper, E. W. Kolb, Z. A. C. Krusberg and T. M. P. Tait, JHEP **1009**, 037 (2010) [arXiv:1002.4137 [hep-ph]].
- [14] P. J. Fox, R. Harnik, J. Kopp and Y. Tsai, Phys. Rev. D **85**, 056011 (2012) [arXiv:1109.4398 [hep-ph]].
- [15] R. C. Cotta, J. L. Hewett, M. P. Le and T. G. Rizzo, arXiv:1210.0525 [hep-ph].
- [16] A. Rajaraman, T. M. P. Tait and A. M. Wijangco, arXiv:1211.7061 [hep-ph].
- [17] A. Read, J. Phys. G: Nucl. Part. Phys. **28**, 2693 (2002);
- [18] T. Junk, Nucl. Instrum. Methods A **434**, 425 (1999).
- [19] J. Alwall, M. Herquet, F. Maltoni, O. Mattelaer and T. Stelzer, JHEP **1106**, 128 (2011) [arXiv:1106.0522 [hep-ph]].